AGU100 ADVANCING EARTH AND SPACE SCIENCE

Geophysical Research Letters

RESEARCH LETTER
10.1029/2019GL085290

Special Section:
New Understanding of the Arabian Sea Circulation

The Impact of Barrier Layers on Arabian Sea Surface Temperature Variability

Rosalind Echols[1] and **Stephen C. Riser**[1]

[1]School of Oceanography, University of Washington, Seattle, WA, USA

Key Points:
- Effect of barrier layers on sea surface temperature in the southeast Arabian Sea varies with season and is nonuniform
- Increased heating associated with barrier layers only significantly observed during northeast monsoon and in isolated patches
- Increased cooling associated with barrier layers during southwest monsoon due to shallower mixed layers increased penetrative radiation

Correspondence to:
R. Echols,
rechols@uw.edu

Citation:
Echols, R., & Riser, S. C. (2020). The impact of barrier layers on Arabian Sea surface temperature variability. *Geophysical Research Letters*, *47*, e2019GL085290. https://doi.org/10.1029/2019GL085290

Received 5 SEP 2019
Accepted 21 JAN 2020
Accepted article online 24 JAN 2020

Abstract Barrier layers (BLs) in the Arabian Sea may lead to increased mixed layer (ML) warming or cooling relative to non-BL conditions, depending on differences in ML properties and atmospheric forcing. We use 13 years of profiling float data from the Arabian Sea to identify when and where each impact is likely based on analysis of the ML temperature tendency. We use a novel method based on the vertical spice profile to identify BLs and their characteristics. BLs are most likely to increase warming during the northeast monsoon, owing to temperature inversions, preceding the development of the miniwarm pool and onset of the southwest monsoon. This effect is nonuniform and is counteracted in some regions by increased penetration of solar radiation below the shallower ML associated with BL. Relative rates of cooling increase in the presence of BL during the southwest monsoon; intermonsoon periods show little net effect from BL.

Plain Language Summary Barrier layers are frequently observed in the world's tropical and subtropical oceans in regions where salinity plays a more important role in determining changes to the upper ocean density than temperature. In the Arabian Sea, where the monsoons affect billions of lives, we wish to understand how the presence of barrier layers may affect the evolution of the upper ocean temperature and thus potentially the behavior of the monsoons. We find significant changes to the mixed layer properties that influence the evolution of sea surface temperature, sometimes leading to increased warming but also frequently leading to increased cooling.

1. Introduction

Barrier layers (BLs) occur when salinity stratification below the density mixed layer (ML) occurs without temperature stratification, producing a barrier between the ML and the cooler waters of the thermocline (Figure 1a; Lukas & Lindstrom, 1991; Sprintall & Tomczak, 1992). Their earliest discovery from high-resolution temperature and salinity profiles in the western Pacific warm pool provided density-based ML depths much shallower than those identified based solely on temperature measurements, arising from the local salinity stratification (Lukas & Lindstrom, 1991). They have subsequently been identified throughout the tropics, including the Bay of Bengal and Arabian Sea (e.g., Sprintall & Tomczak, 1992), where massive transport of freshwater from rivers establishes strong salinity stratification near the surface. Their departure from a thermally stratified ML base raises questions about their impact on sea surface temperatures (SST).

In the southeast Arabian Sea (SEAS), where high SSTs have been observationally linked to the southwest monsoon onset (Rao & Sivakumar, 1999; Shenoi et al., 1999), models show evidence of enhanced warming associated with BLs during the spring intermonsoon prior to monsoon onset (Masson et al., 2005). Shallower MLs may support increased warming and momentum transfer due to heat fluxes and wind stress being absorbed in a thinner layer (Cronin & Kessler, 2009; Cronin & McPhaden, 2002); modification of the stratification below the ML can alter wind-driven mixing (Niiler & Kraus, 1977), and the separation between the density ML and the thermocline may alter the consequences of mixing. Strong salinity stratification allows the upper ocean to support substantial temperature inversions without convective overturn (Kurian & Vinayachandran, 2006; Shankar et al., 2004; Vinayachandran et al., 2007).

Yet it should not be a foregone conclusion that BL presence results in increased ML warming. Vinayachandran et al. (2007) proposed that shallow MLs subjected to net heat flux from ocean to atmosphere may in fact lead to enhanced cooling, although at the time there was insufficient data to fully investigate this hypothesis. The Arabian Sea is a complex region, with seasonally reversing currents (Schott &

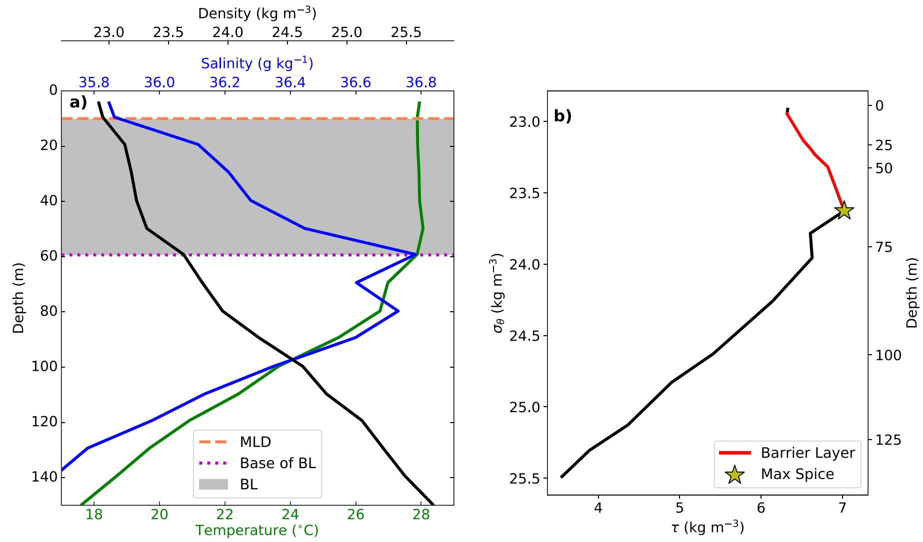

Figure 1. (a) Temperature (green), salinity (blue), and density (black) profiles indicating presence of a barrier layer BL (gray shading). Base of mixed layer (orange) and BL (magenta) indicated by dashed lines. (b) Plot of density versus spice for profile shown in (a). Red line indicates the BL.

McCreary, 2001), upwelling, downwelling, and widely varying seasonal and regional heat flux, making a simple statement about BL impact impossible. In addition, modeling studies sometimes overestimate ML depth associated with BL (Masson et al., 2005) and often have lower vertical resolution than is available with modern observational techniques. Given the range of possible BL impacts, nuances in the differences between BL and non-BL profiles may be significant to their impact.

Here, we use 13 years of Argo float data to examine the impact of BL in the SEAS by comparing the characteristics of BL and non-BL profiles and examining how differences in these characteristics impact relevant terms of the ML temperature tendency equation. The study benefits from greater data density and wider data distribution than previous observational studies, a method for identifying BL that more precisely captures ML and BL characteristics, and greater vertical resolution in the data than previous modeling studies.

2. Data

This study uses Argo-type float data spanning the years 2004–2016, starting when the float distribution reached approximately full spatial and temporal coverage in the region and ending when this study began. Floats typically spend ~9 days at a parking depth near 1,000 m before descending to 2,000 m and profiling upward to the surface, achieving a vertical measurement resolution of ~2 m near the surface (Riser et al., 2016). We focus on the SEAS, here considered to be the region bounded by the equator and 15°N, spanning longitudes of 60°E and 80°E (Figure 2, red outlines). Initially, all available temperature (T) and salinity (S) profiles were considered. Any profile with missing temperature or salinity data in the top 10 m was discarded, as well as profiles with values outside a reasonable range for this location ($0 < T < 35$ °C and $20 < S < 40$). Profiles whose maximum pressure was less than 100 m, or with large gaps in the pressure data, were also excluded. After these quality control measures, there were a total of 13,923 useable profiles of temperature and salinity (~66% of the original total). In contrast with previous observational studies (e.g., de Boyer Montégut et al., 2014; Thadathil et al., 2008), data coverage is better across the eastern and southern portions of the region (>50 profiles seasonally per 2° × 2° box outside of coastal and shallow regions). The monthly average number of total float profiles is roughly even between months, although there is some interannual variability (Figure 2).

Daily averaged heat fluxes and wind fields from the National Centers for Environmental Prediction/Department of Energy Reanalysis (version 2) were used to calculate approximate fluxes associated with individual profiles (Kanamitsu et al., 2002). While the lack of collocated measurements (such as those from shipboard measurements) poses a challenge for making precise calculations associated with

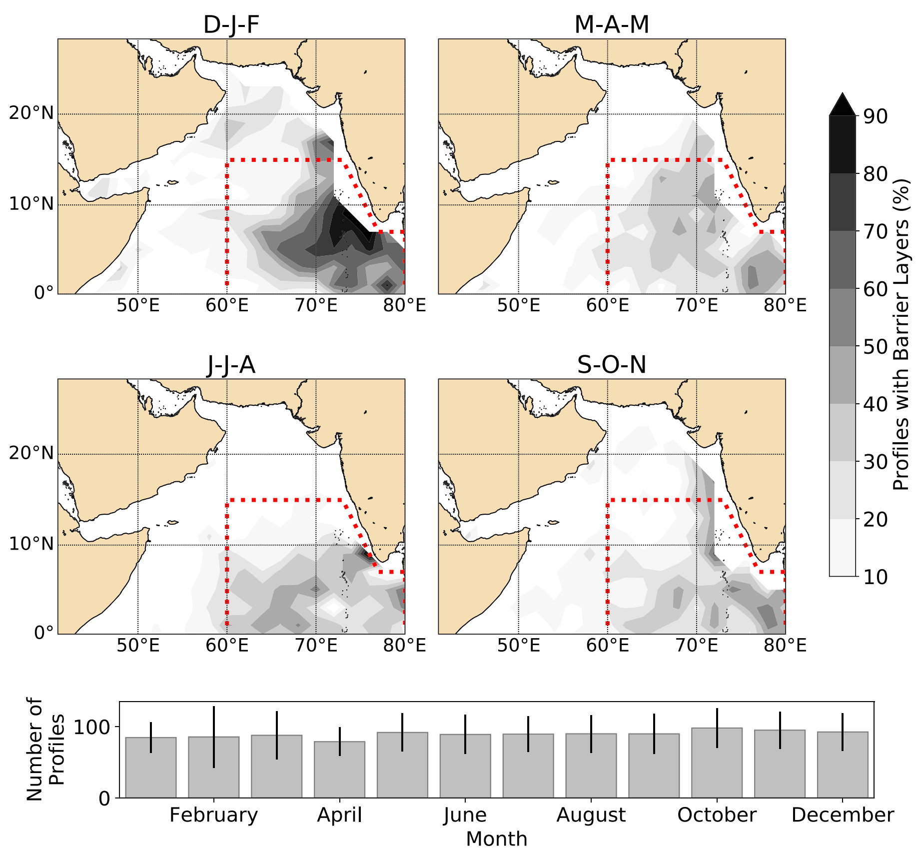

Figure 2. Barrier layer frequency by season. Red-dashed area indicates southeast Arabian Sea—definition used in this study. D-J-F is the northeast monsoon, December–February; M-A-M is the spring intermonsoon, March–May; J-J-A is the southwest monsoon, July–August; and S-O-N is the fall intermonsoon, September–November. Bottom panel shows average monthly number of profiles in study area; error bars indicate standard deviation across all years.

an individual profile, the goals of this study are to understand bulk regional impacts of BLs in the SEAS, and these data provide a reasonable starting point.

3. Methods

As defined by Lukas and Lindstrom (1991), the BL is the layer between the base of the density ML and the top of the thermocline that exists due to strong salinity stratification (Figure 1a). Rather than considering a temperature threshold to define the end of the BL, we consider diapycnal changes in spice, a state variable that allows simultaneous consideration of temperature and salinity (Flament, 2002; Jackett & McDougall, 1985; Shcherbina et al., 2009; Veronis, 1972). An approximate differential form of spice is

$$d\tau = \rho(\alpha d\theta + \beta dS), \tag{1}$$

where τ denotes spice, ρ is the reference density, θ is potential temperature, $\alpha = -\frac{1}{\rho}\left(\frac{\partial \rho}{\partial \theta}\right)$, and $\beta = \frac{1}{\rho}\left(\frac{\partial \rho}{\partial S}\right)$ (Shcherbina et al., 2009). BLs exist when lower density, fresh (and sometimes cooler) water (low spice) overlays higher density salty (and sometimes warmer) water (high spice) (Echols & Riser, 2020). The top of the thermocline, and base of the BL, coincides with the reverse transition in spice. In this framework, the base of the ML is defined as the depth of the first diapycnal transition from lower to higher spice (beginning of salinity-controlled stratification), and the base of the BL is defined as the diapycnal transition from higher to lower spice (temperature-controlled stratification) (Figure 1b; Echols & Riser, 2020). We use the shallow water definition of spiciness described in McDougall and Krzysik (2015) to quantitatively determine spice. This definition accommodates variations in the strength of temperature and salinity stratification without selecting a different temperature threshold and identifies the depth of the appropriate transition rather than the depth where a threshold has been exceeded. Figure 2 shows the seasonal BL frequency determined from this method. BL frequency is the value R used by Mignot et al. (2009) to calculate porosity $(1 - R)$, although without the same restrictions on BL thickness.

To investigate the evolution of SST through interactions with the atmosphere, with and without BLs present, we focus on the particular terms in an ML temperature tendency equation (Foltz et al., 2003; McPhaden & Hayes, 1991; Stevenson & Niiler, 1983) that may be affected by the changes to the ML associated with BLs. Assuming that temperature and velocity are both constant over the ML depth, we use

$$\underset{(a)}{\frac{\partial T}{\partial t}} + \underset{(b)}{(\mathbf{v}\cdot\nabla T)} + \underset{(c)}{\frac{(T_{\mathrm{ML}}-T_{-h})w_e}{h}} = \underset{(d)}{\frac{q_0-q_{-h}}{h\rho c_p}}, \tag{2}$$

where $\mathbf{v}$ represents the horizontal velocity within the ML, T_{ML} is the vertically averaged ML temperature, T_{-h} is the temperature just below the base of the ML (here taken as 10 m below the bottom of the ML), h is the ML depth, and w_e is the entrainment velocity. Term (a) represents the temperature tendency; (b) advection by the mean flow; (c) entrainment of water below the ML; and (d) heat flux into the ML, in which the total surface heat flux (q_0) is decreased by the heat flux due to shortwave radiation penetrating downwards through the base of the ML and turbulent mixing (q_{-h}). For the purposes of this study, we focus solely on the penetrative radiation component of q_{-h} and incorporate turbulent mixing into the calculation of w_e (see equation (4)). Given the data available for this study, which do not include horizontal velocities tied to specific float profiles, and previous work showing that advection was not a dominant term in the heat budget (Durand et al., 2004; Rao & Sivakumar, 1999), we will only evaluate terms (a), (c), and (d) in considering the impacts of BLs.

For shallow MLs, and typical tropical heat fluxes, the radiation penetrating the base of the ML in term (d), q_{-h}, could significantly reduce the heat transfer to the ML. In an ideal BL, the ML resides within a completely isothermal layer, so term *(c)* would be identically 0, unlike the cooling we might expect with a temperature-stratified ML. Figure 1a shows an example profile where T_{ML} does not differ significantly from T_{-h}; even for BL profiles that deviate from this model and have slight temperature stratification, we expect this term to be much smaller than in a normal ML and likely negligible if T_{-h} is very close to T_{ML} (Vialard & Delecluse, 1998). These effects may exert opposing influences on SST.

Temperature inversions, where the temperature at depth exceeds SST by at least 0.2 °C, can also develop during the lifetime of the BL (Kurian & Vinayachandran, 2006) due to surface cooling under negative heat flux conditions (term (d) in equation (2) is negative, implying net heat flux out of the ML). Significant temperature inversions are only possible if the salinity stratification is strong enough to compensate for the density changes associated with increased temperature, that is, if $\beta dS > \alpha dT$, (where $\alpha = -\frac{1}{\rho}\left(\frac{\partial\rho}{\partial T}\right)$ and $\beta = \frac{1}{\rho}\left(\frac{\partial\rho}{\partial S}\right)$); otherwise, convective overturn would lead to BL erosion. Temperature inversions have been observed in the SEAS during the northeast monsoon (Durand et al., 2004; Shankar et al., 2004; Vinayachandran et al., 2007). Therefore, term (c) could also contribute a positive tendency to the SST change when $T_{-h} > T_{ML}$ (Durand et al., 2004; Shankar et al., 2004; Smyth et al., 1996). Differences in ML depth, h, could further alter the impact of terms (c) and (d) owing to its position in the denominator.

Several models exist for determining the penetrative radiation at the base of the ML. For the Arabian Sea, BLs are most commonly found in the low chlorophyll southeastern regions (Sweeney et al., 2005; Figure 2), and profiling floats rarely enter the near-coastal waters of western India where productivity (and thus chlorophyll) can be elevated. Therefore, here we use a simple parameterization with a constant extinction coefficient of $\gamma = 0.04\ \mathrm{m}^{-1}$ corresponding to a 25-m e-folding depth (Foltz et al., 2003; Niiler & Kraus, 1977; Wang & McPhaden, 1999) to estimate q_{-h} using

$$q_{-h} = 0.45 q_{\mathrm{short}} e^{-\gamma h}, \tag{3}$$

where q_{short} is the net surface shortwave heat flux. Values of the coefficient, which describes the fraction of light penetrating past the uppermost few meters, range between 0.42 and 0.47 across studies of tropical regions, so we follow Wang and McPhaden (1999) in using 0.45.

Lacking direct measurements of the vertical velocity, estimating the entrainment velocity, w_e, is difficult. Fully assessing w_e from the turbulent kinetic energy balance requires consideration of free convection, shear flow, vertical turbulent energy flux, and dissipation (Niiler & Kraus, 1977). Data required for investigation of shear effects or dissipation are not available for this region; to approximate w_e, we instead use an expression to estimate the effects of wind work without any buoyancy effects, after McPhaden and Hayes (1991).

$$w_e = \frac{2m\left(\frac{\rho_a C_D}{\rho_0}\right)^{3/2}|U|^3}{-g\left(\frac{\rho}{\rho_0}\right)h}, \tag{4}$$

where m is an efficiency factor (Niiler & Kraus, 1977); ρ_0 is the ML density; ρ is the jump in density across the base of the ML; g is gravity; and ρ_a, C_D, and U are the air density, drag coefficient, and wind velocity, respectively. The presence of a BL could modify this term through changes to ρ or ML depth. Entrainment is only relevant for cases of ML deepening, where water below the ML might be incorporated into the ML; for values that might suggest ML shoaling, we neglect it. We also examine changes to the ML depth, $\frac{\partial h}{\partial t}$, estimated from the change in ML between float profiles divided by the time between the profiles, as well as the formulation used by Lee et al. (2000), which includes buoyancy effects. Because floats sometimes move between water masses, the former calculation is not completely reliable for determining ML deepening. However, all three methods show comparable values and seasonal cycles.

4. Results

Basin-wide, the presence of BLs is associated with differences in the depth of the ML and the stratification immediately below it; the greatest difference between BL and non-BL conditions is observed during the southwest and northeast monsoons (Figure 3). In comparison with MLs determined by temperature stratification, BLs are typically associated with lower stratification below the ML (Figure 3a) and shallower MLs (Figure 3b). This produces greater rates of ML deepening (Figure 3c) because there is lower resistance to wind work (equation (4)). Regions with strong BL presence (as in Figure 2) are typically associated with a 15–25 W m^{-2} increase in average penetrative radiation, q_{-h} (Figure 3d), implying less heat flux into the ML and more downward heat flux below the ML. This effect is most pronounced during the northeast monsoon where BLs are most frequent (not shown).

Figure 3e shows the impact of BLs on term (c) (temperature change due to entrainment) in equation (1). Entrainment cooling is greatly reduced in the presence of a BL. During the northeast monsoon (December and January), the entrainment term tends to be positive for BL profiles. The magnitude of the effect depends slightly on the depth below the ML used for T_{-h} and the method used to calculate w_e. However, all methods produced comparable estimates. The small positive values observed in December and January in Figure 3e for the BL line are consistent with the occurrence of temperature inversions during the winter monsoon (Durand et al., 2004). The temperature inversions observed here average $T \approx 0.4\ ° C$ above T_{ML} during the northeast monsoon in the SEAS, accounting for roughly 23% of all profiles (34% if the restricted SEAS definition employed by previous studies is used; Durand et al., 2004). Although most temperature inversions fall in the range $0.2\ ° C \leq T \leq 0.5\ ° C$, occasionally BLs are observed with T~1.0 ° C. This is consistent with work showing negative atmospheric heat fluxes in some parts of the region where BLs are formed (Shankar et al., 2004; Thadathil & Gosh, 1992; Thompson et al., 2006). Float data indicate that temperature inversions can persist for two or more consecutive profiles during the northeast monsoon (>20 days), emphasizing the importance of considering this term on seasonal time scales. The values in Figure 3e may overestimate the amount of cooling given that the monthly values are determined by assuming that the ML deepening persists for an entire month. However, qualitatively, these terms confirm that the presence of a BL significantly reduces entrainment cooling and could even contribute to ML warming instead of cooling in the northeast monsoon season, potentially preconditioning the ML for the subsequent warming during the intermonsoon period (March–May) (Durand et al., 2004).

Figure 3f depicts the impact of BLs on the heat flux (term (d)). Consistent with the shallower ML and therefore increased penetrative radiation, BLs tend to have a cooling effect relative to non-BL when

10.1029/2019GL085290

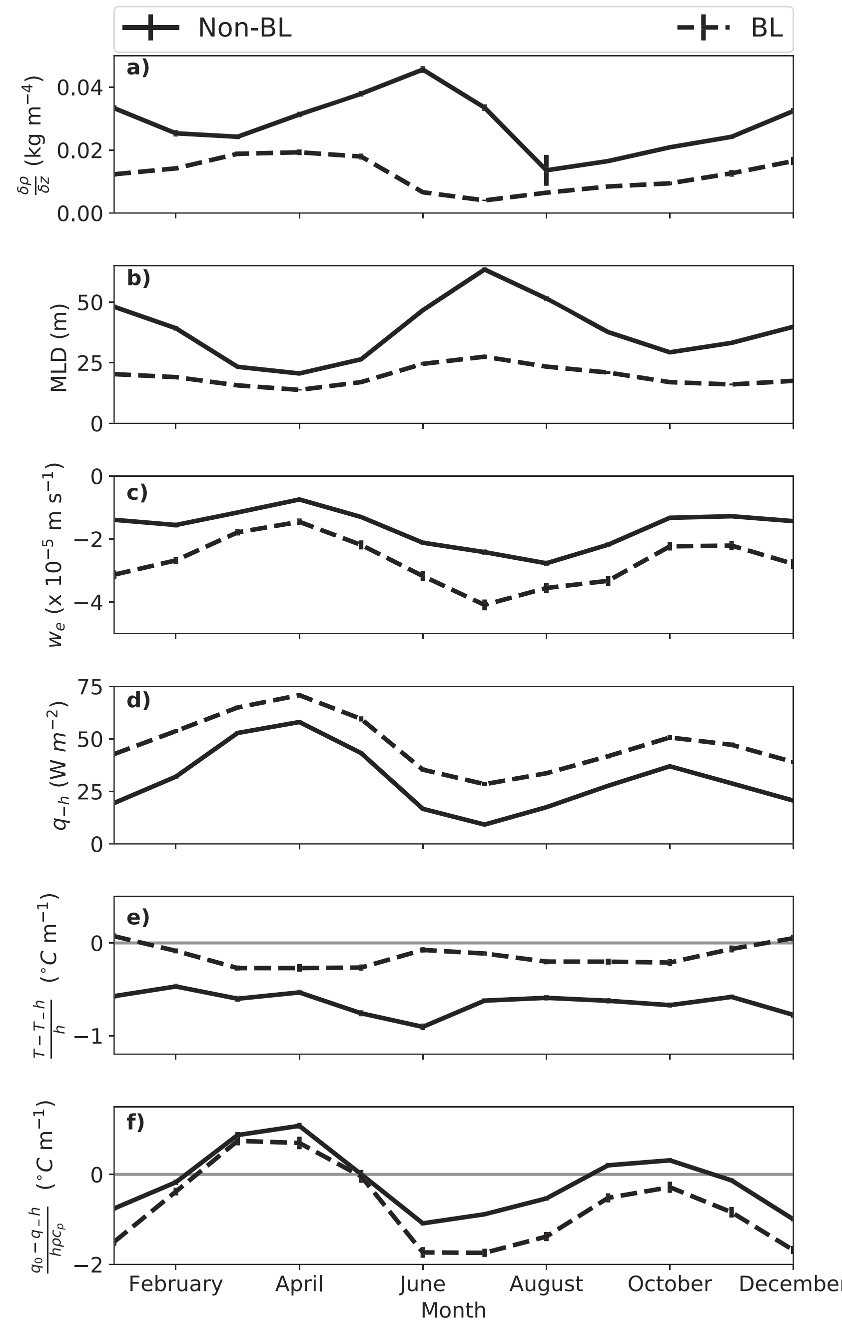

Figure 3. Comparison of mixed-layer characteristics in the southeast Arabian Sea between barrier layer (BL) and non-BL profiles: (a) Stratification below the ML; (b) ML depth; (c) entrainment velocity (equation (3)); (d) penetrative radiation; (e) monthly change in temperature due to entrainment mixing; and (f) monthly change in temperature due to heat flux.

considering the heat flux. However, the extent of the difference varies by season. The spring intermonsoon shows the smallest difference; combined with the decrease in entrainment cooling, this suggests increased warming as a result of the presence of BL, potentially significant leading up to the onset of the southwest monsoon. The greatest difference occurs during the southwest monsoon and into the fall, where the presence of BL is associated with a shift from a net warming to net cooling. BLs are less common during the fall intermonsoon than either the northeast or southwest monsoon, so their presence is unlikely to lead to cooling; however, their presence may damp the heating otherwise expected during this season.

10.1029/2019GL085290

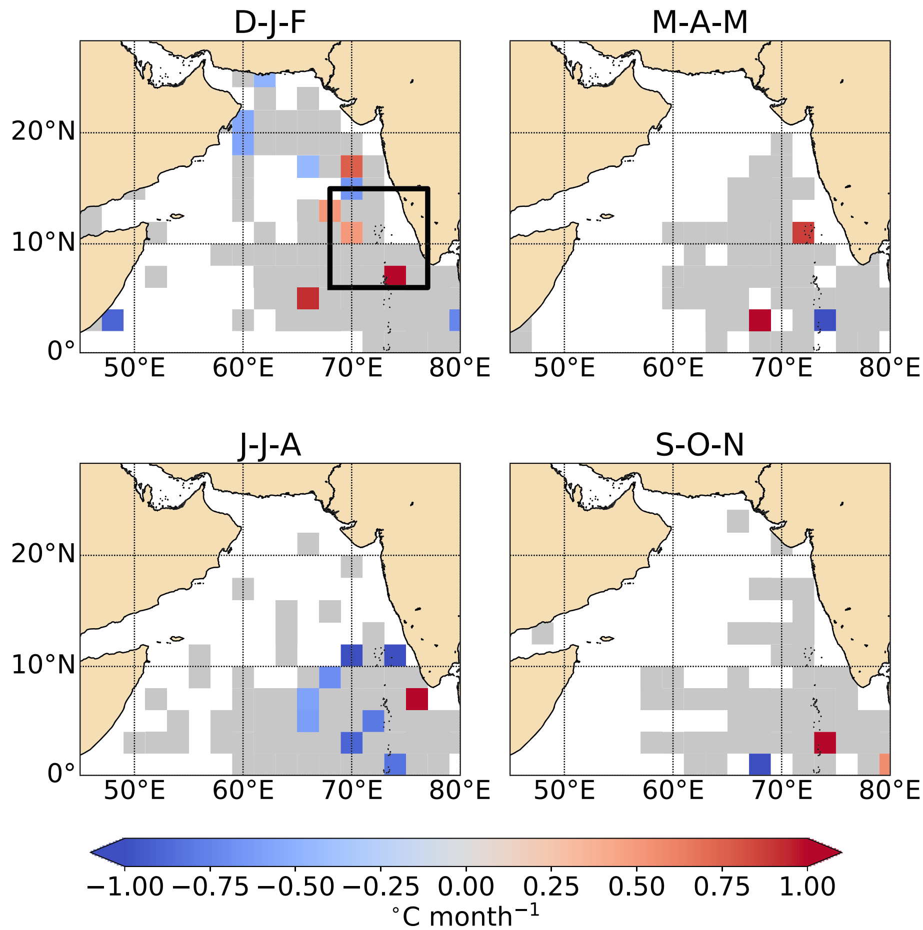

Figure 4. Difference in monthly net heating rate between BL and non-BL profiles: $\frac{\partial T}{\partial t}_{\mathrm{BL}} - \frac{\partial T}{dt}_{\mathrm{non-BL}}$. Red (blue) shading indicates increased (decreased) warming or decreased (increased) cooling associated with presence of BL. Gray regions indicate areas where BL are common, but difference between BL and non-BL is not statistically significant ($p > 0.05$).

Figure 4 shows the difference between the temperature tendency resulting from terms (*c*) and (*d*) for BL and non-BL cases in 2° × 2° boxes. Positive (negative) values indicate increased (decreased) warming or decreased (increased) cooling associated with BL compared with non-BL. Figure 4 indicates that the effects summarized by Figure 3 are localized and not uniform throughout the SEAS. In agreement with Durand et al. (2004), we find a warming signal off the west coast of India, coincident with where BLs are most frequent (Figure 2) and temperature inversions the strongest. The locations of significant relative warming values coincide with a positive sum of terms (*c*) and (*d*) for the BL cases (not shown) and indicate increased warming on the order of >0.5 °C month^{-1}.

Cooling is more likely during the southwest monsoon, which reflects the large difference in ML depth between BL and non-BL profiles (Figure 3b). The pattern of cooling, while not significant everywhere, is distributed throughout the region where BL typically constitutes more than 40% of the profiles and is on the order of 0.5 °C month^{-1}. Despite strong positive atmospheric heat flux during the spring and fall intermonsoon seasons, we did not encounter a significant increase in the expected warming associated with the presence of BL possibly because the decreased entrainment cooling is offset by decreased absorption of heat within the ML for most of the basin.

5. Discussion

Several hypotheses relating to the impact of BL on SST have been previously proposed: warming (e.g., Durand et al., 2004; Lukas & Lindstrom, 1991; Masson et al., 2005), cooling (Vinayachandran et al., 2007), and insulation of the ML from atmospheric forcing (Vialard & Delecluse, 1998). This work illustrates that all of these effects may occur within the same region depending on the atmospheric fluxes and characteristics of the ML. Increased warming or decreased cooling may occur in the presence of BL during the northeast monsoon (where temperature inversions are most common) and spring intermonsoon (where differences in the impact of the heat flux are minimum), but increased cooling is likely during the southwest monsoon when ML depth differences are maximized. However, in many cases, there is not a statistically significant difference between the BL and non-BL cases (gray shading, Figure 4), despite significant differences in the individual ML characteristics and terms in the temperature tendency equation (Figure 3). The magnitude of the increased warming is smaller than that determined from modeling studies (e.g., Durand et al., 2004), perhaps due to the lack of near-coast data (where temperature inversions are most frequent) or differences in observed ML depth.

BLs are conducive to enhanced nighttime cooling of the ML during transient negative surface heat flux and also longer-term cooling due to the strong, sustained salinity stratification. Changes to the ML temperature are a significant factor in determining the magnitude of temperature inversions, where cooling at the surface traps warmer water below. In the long term, this may negate some of the additional cooling allowed by the BL at the surface through vertical entrainment but is unlikely to fully compensate the effects of large net heat loss at the surface when BLs are present. The statistically insignificant difference in BL and non-BL scenarios illustrated in Figure 4 suggests that the warming and cooling effects of BL may be counteracting one another, as suggested by Vialard and Delecluse (1998).

Penetrative radiation in this region is large in comparison with the net surface heat flux. This plays a critical role in determining differences between BL and non-BL scenarios. Other studies in this area identified comparable values of q_{-h} (e.g., Sengupta et al., 2008), but its contribution to the overall temperature tendency warrants additional investigation. The use of a constant extinction coefficient in equation (3) may lead to overestimates of q_{-h}, likely underestimating any increase in warming associated with BL. Furthermore, while advective processes certainly play a role in forming BL in this region (e.g., Durand et al., 2007), it remains to be seen how the presence of BL may influence advective changes to SST. While each of these may be worth investigating, they are likely to be of lower significance than the first-order approximation calculated here.

Finally, the work here has focused on seasonal patterns based on temporal and spatial averages. However, one-dimensional modeling studies (e.g., Shinoda, 2005) have demonstrated the importance of diurnal cycles in affecting intraseasonal variations in SST. These studies show differences in SST when hourly data are used to calculated temperature changes rather than daily averaged (as used here). However, the majority of these studies have been conducted on thermally stratified ML and thus show ML deepening at night that is unlikely to occur in the presence of BL. Transient temperature inversions associated with nighttime cooling are possible in the presence of BL. This suggests that diurnal cycles (and their impacts on intraseasonal SST variation) may differ in the presence of BL; for a study of those processes, a different data set would be required.

Acknowledgments
We thank K. Drushka, M. Cronin, and three anonymous reviewers for their feedback and suggestions. This material is based upon work supported by the National Science Foundation Graduate Research Fellowship Program under Grant DGE-1762114. Any opinions, findings, and conclusions or recommendations expressed in this material are those of the author(s) and do not necessarily reflect the views of the National Science Foundation. We also gratefully acknowledge the generous support of Office of Naval Research through NASCar Grant N00014-15-1-2254 and NOAA Grant NA15OAR4320063 to the University of Washington, through the Joint Institute for the Study of the Ocean and the Atmosphere. These data were collected and made freely available by the International Argo Program and the national programs that contribute to it (http://www.argo.ucsd.edu and http://argo.jcommops.org). The Argo Program is part of the Global Ocean Observing System. NCEP/DOE 2 reanalysis data are provided by the NOAA/OAR/ESRL PSD, Boulder, Colorado, USA, from their Web site (https://www.esrl.noaa.gov/psd/).

References

Cronin, M. F., & Kessler, W. S. (2009). Near-surface shear flow in the tropical Pacific cold tongue front. *Journal of Physical Oceanography*, *39*(5), 1200–1215. https://doi.org/10.1175/2008JPO4064.1

Cronin, M. F., & McPhaden, M. J. (2002). Barrier layer formation during westerly wind bursts. *Journal of Geophysical Research*, *107*(C12), 8020. https://doi.org/10.1029/2001JC001171

de Boyer Montégut, C., Durand, F., Bourdallé-Badie, R., & Blanke, B. (2014). Role of fronts in the formation of Arabian Sea barrier layers during summer monsoon. *Ocean Dynamics*, *64*(6), 809–822. https://doi.org/10.1007/s10236-014-0716-7

Durand, F., Shankar, D., de Boyer Montégut, C., Shenoi, S. S. C., Blanke, B., & Madec, G. (2007). Modeling the barrier layer formation in the southeastern Arabian Sea. *Journal of Climate*, *20*(10), 2109–2120. https://doi.org/10.1175/JCLI4112.1

Durand, F., Shetye, S. R., Vialard, J., Shankar, D., Shenoi, S. S. C., Ethe, C., & Madec, G. (2004). Impact of temperature inversions on SST evolution in the south-eastern Arabian Sea during the pre-summer monsoon season. *Geophysical Research Letters*, *31*, L01305. https://doi.org/10.1029/2003GL018906

Echols, R., & Riser, S. C. (2020). Spice and barrier layers: An Arabian Sea case study. *Journal of Physical Oceanography*, *in press*, JPO-D-19-0215.1. https://doi.org/10.1175/JPO-D-19-0215.1

Flament, P. (2002). A state variable for characterizing water masses and their diffusive stability: Spiciness. *Progress in Oceanography*, *54*(1-4), 493–501. https://doi.org/10.1016/S0079-6611(02)00065-4

Foltz, G. R., Grodsky, S. A., Carton, J. A., & McPhaden, M. J. (2003). Seasonal mixed layer heat budget of the tropical Atlantic Ocean. *Journal of Geophysical Research*, *108*(C5), 3146. https://doi.org/10.1029/2002JC001584

Jackett, D. R., & McDougall, T. J. (1985). An oceanographic variable for the characterization of intrusions and water masses. *Deep Sea Research*, *32*(10), 1195–1207. https://doi.org/10.1016/0198-0149(85)90003-2

Kanamitsu, M., Ebisuzaki, W., Woollen, J., Yang, S.-K., Hnilo, J. J., Fiorino, M., & Potter, G. L. (2002). NCEP-DOE AMIP-II reanalysis (R-2). *Bulletin of the American Meteorological Society*, *83*(11), 1631–1644. https://doi.org/10.1175/BAMS-83-11-1631

Kurian, J., & Vinayachandran, P. N. (2006). Formation mechanisms of temperature inversions in the southeast Arabian Sea. *Geophysical Research Letters*, *33*, L17611. https://doi.org/10.1029/2006GL027280

Lee, C. M., Jones, B. H., Brink, K. H., & Fischer, A. S. (2000). The upper-ocean response to monsoonal forcing in the Arabian Sea: Seasonal and spatial variability. *Deep-Sea Researh II*, *47*(7-8), 1177–1226. https://doi.org/10.1016/S0967-0645(99)00141-1

Lukas, R., & Lindstrom, E. (1991). The mixed layer of the western equatorial Pacific Ocean. *Journal of Geophysical Research*, *96*(S01), 3343–3357. https://doi.org/10.1029/90JC01951

Masson, S., Luo, J.-J., Madec, G., Vialard, J., Durand, F., Gualdi, S., et al. (2005). Impact of barrier layer on winter-spring variability of the southeastern Arabian Sea. *Geophysical Research Letters*, *32*, L07703. https://doi.org/10.1029/2004GL021980

McDougall, T. J., & Krzysik, O. A. (2015). Spiciness. *Journal of Marine Research*, *73*(5), 141–152. https://doi.org/10.1357/002224015816665589

McPhaden, M. J., & Hayes, S. P. (1991). On the variability of winds, sea surface temperature, and surface layer heat content in the western equatorial Pacific. *Journal of Geophysical Research*, *96*(S01), 3331–3342. https://doi.org/10.1029/90JC01726

Mignot, J., de Boyer Montégut, C., & Tomczak, M. (2009). On the porosity of barrier layers. *Ocean Science*, *5*(3), 379–387. https://doi.org/10.5194/os-5-379-2009

Niiler, P. P., & Kraus, E. B. (1977). One-dimensional models of the upper ocean. In E. B. Kraus (Ed.), *Modelling and prediction of the upper layers of the ocean*, (pp. 143–172). New York: Pergamon.

Rao, R. R., & Sivakumar, R. (1999). On the possible mechanisms of the evolution of a mini-warm pool during the pre-summer monsoon season and the genesis of onset vortex in the south-east Arabian Sea. *Quarterly Journal of the Royal Meteorological Society*, *125*(555), 787–809. https://doi.org/10.1002/qj.49712555503

Riser, S. C., Freeland, H. J., Roemmich, D., Wijffels, S., Troisi, A., & Belbéoch, M. (2016). Fifteen years of ocean observations with the global Argo array. *Nature Climate Change*. Nature Publishing Group., *6*(2), 145–153. https://doi.org/10.1038/nclimate2872

Schott, F. A., & McCreary, J. P. (2001). The monsoon circulation of the Indian Ocean. *Progress in Oceanography*, *51*(1), 1–123. https://doi.org/10.1016/S0079-6611(01)00083-0

Sengupta, D., Parampil, S. R., Bhat, G. S., Murty, V. S. N., Ramesh Babu, V., Sudhakar, T., et al. (2008). Warm pool thermodynamics from the Arabian Sea monsoon experiment (ARMEX). *Journal of Geophysical Research*, *113*, C10008. https://doi.org/10.1029/2007JC004623

Shankar, D., Gopalakrishna, V. V., Shenoi, S. S. C., Durand, F., Shetye, S. R., Rajan, C. K., et al. (2004). Observational evidence for westward propagation of temperature inversions in the southeastern Arabian Sea. *Geophysical Research Letters*, *31*, L08305. https://doi.org/10.1029/2004GL019652

Shcherbina, A. Y., Gregg, M. C., Alford, M. H., & Harcourt, R. R. (2009). Characterizing thermohaline intrusions in the North Pacific subtropical frontal zone. *Journal of Physical Oceanography*, *39*, 2735–2756. https://doi.org/10.1175/2009JPO4190.1

Shenoi, S. S. C., Shankar, D., & Shetye, S. R. (1999). On the sea surface temperature high in the Lakshadweep Sea before the onset of the southwest monsoon. *Journal of Geophysical Research*, *104*(C7), 15,703–15,712. https://doi.org/10.1029/1998JC900080

Shinoda, T. (2005). Impact of the Diurnal Cycle of Solar Radiation on Intraseasonal SST Variability in the Western Equatorial Pacific. *Journal of Climate*, *18*(14), 2628–2636. https://doi.org/10.1175/jcli3432.1

Smyth, W. D., Hebert, D., & Moum, J. N. (1996). Local ocean response to a multiphase westerly wind burst: 2. Thermal and freshwater responses. *Journal of Geophysical Research*, *101*(C10), 22,513–22,533. https://doi.org/10.1029/96JC02006

Sprintall, J., & Tomczak, M. (1992). Evidence of the barrier layer in the surface layer of the tropics. *Journal of Geophysical Research*, *97*(C5), 7305–7316. https://doi.org/10.1029/92JC00407

Stevenson, J. W., & Niiler, P. P. (1983). Upper ocean heat budget during the Hawaii-to-Tahiti shuttle experiment. *Journal of Physical Oceanography*, *13*(10), 1894–1907. https://doi.org/10.1175/1520-0485(1983)013<1894:UOHBDT>2.0.CO;2

Sweeney, C., Gnanadesikan, A., Griffies, S. M., Harrison, M. J., Rosati, A. J., & Samuels, B. L. (2005). Impacts of shortwave penetration depth on large-scale ocean circulation and heat transport. *Journal of Physical Oceanography*, *35*(6), 1103–1119. https://doi.org/10.1175/JPO2740.1

Thadathil, P., & Gosh, A. K. (1992). Surface layer temperature inversions in the Arabian Sea during winter. *Journal of Oceanography*, *48*(3), 293–304. https://doi.org/10.1007/BF02233989

Thadathil, P., Thoppil, P., Rao, R. R., Muraleedharan, P. M., Somayajulu, Y. K., Gopalakrishna, V. V., et al. (2008). Seasonal variability of the observed barrier layer in the Arabian Sea. *Journal of Physical Oceanography*, *38*(3), 624–638. https://doi.org/10.1175/2007JPO3798.1

Thompson, B., Gnanaseelan, C., & Salvekar, P. S. (2006). Seasonal evolution of temperature inversions in the north Indian Ocean. *Current Science*, *90*(5), 697–704.

Veronis, G. (1972). On properties of seawater defined by temperature, salinity, and pressure. *Journal of Marine Research*, *30*(2), 227–255.

Vialard, J., & Delecluse, P. (1998). An OGCM study for the TOGA decade. Part 1: Role of salinity in the physics of the western Pacific fresh pool. *Journal of Physical Oceanography*, *28*(6), 1071–1088. https://doi.org/10.1175/1520-0485(1998)028<1071:AOSFTT>2.0.CO;2

Vinayachandran, P., Shankar, D., Kurian, J., Durand, F., & Shenoi, S. S. C. (2007). Arabian Sea mini warm pool and the monsoon onset vortex. *Current Science*, *93*(2), 203–214.

Wang, W., & McPhaden, M. J. (1999). The surface-layer heat balance in the equatorial Pacific Ocean. Part 1: Mean seasonal cycle. *Journal of Physical Oceanography*, *29*(8), 1812–1831. https://doi.org/10.1175/1520-0485(1999)029<1812:TSLHBI>2.0.CO;2